Polarized-neutron reflectivity for thin films of dilute magnetic alloys

V. N. Gladilin,* V. M. Fomin,*,† and J. T. Devreese†
Theoretische Fysica van de Vaste Stoffen, Departement Natuurkunde, Universiteit Antwerpen, Universiteitsplein 1, B-2610 Antwerpen, Belgium

J. Swerts, K. Temst, and C. Van Haesendonck
Laboratorium voor Vaste-Stoffysica en Magnetisme, Katholieke Universiteit Leuven, Celestijnenlaan 200 D, B-3001 Leuven, Belgium
(Received 7 July 2003; revised manuscript received 12 February 2004; published 18 October 2004)

We analyze the influence of the surface-induced anisotropy of magnetic-impurity spins on the magnetization of thin polycrystalline films, consisting of weakly-coupled grains of homogeneous dilute magnetic alloys. The calculated magnetization depth profiles across such AuFe films appear to be very sensitive to the grain shape. Based on these calculations, we theoretically study the reflection of polarized neutrons by AuFe films with different microstructure and show that polarized-neutron reflectivity measurements can provide a direct probe of the surface-induced magnetic anisotropy of the impurity spins in films of dilute magnetic alloys.

DOI: 10.1103/PhysRevB.70.144408 PACS number(s): 75.20.Hr, 75.30.Gw, 75.25.+z

I. INTRODUCTION

Experiments on mesoscopic samples of dilute magnetic alloys[1–6] revealed a vast variety of size effects in the Kondo resistivity, the thermopower, and the Hall resistivity of these samples. In Refs. 7–9 size-dependent Kondo scattering was linked to the surface-induced anisotropy of magnetic-impurity spins. As shown in Refs. 7–9, the spin of an impurity, embedded in a semi-infinite nonmagnetic host matrix, tends to be aligned parallel to the host surface. This anisotropy results from the interaction of the impurity spin with conduction electrons that undergo spin-orbit scattering by host atoms. The theory of the surface-induced anisotropy in dilute magnetic alloys has been further generalized[6,10–12] for arbitrary geometry of samples. In particular, it has been shown[6,11,12] that impurity-spin states and the corresponding impurity-spin magnetization in polycrystalline films, consisting of weakly coupled grains of homogeneous dilute magnetic alloys, are very sensitive to the grain shape as well as to the specific positions of the impurities within a grain.

Neutron reflectivity has emerged as one of the most powerful techniques to study the magnetization profile and magnetization directions of thin ferromagnetic and superconducting films. The reflection of neutrons from a thin film can be described using an optical formalism that is governed by the refractive index of the thin film material. Similar to the reflection of x rays, this formalism can be easily extended to the reflection from a multilayered thin film sample. On the other hand, neutron reflectivity is complementary to x-ray reflectivity due to the fact that the neutron-scattering length is not increasing monotonously with the atomic number. Moreover, neutrons carry a magnetic moment, which can interact with the local magnetic induction. For polarized neutrons the refractive index depends on the nuclear and the magnetic neutron-sample interactions. A different refractive index for neutron spin parallel or antiparallel to an external neutron guide field leads to different reflectivities for a spin-up neutron beam (denoted by R^+) and a spin-down neutron beam (denoted by R^-). The difference between the spin-up reflectivity R^+ and the spin-down reflectivity R^- can be related to the sample magnetization. Comparison with an optical model, which takes into account the neutron spin-dependent reflectivity, allows one to reconstruct a magnetic depth profile[14,15] that is not available for standard inductive magnetization measurements, such as SQUID magnetometry. Neutron reflectivity has been successfully used to study the penetration of vortices and the magnetic penetration depth in thin superconducting films.[16,17] It also played an important role in the elucidation of the magnetic structure in magnetic heterostructures.[18] More recently, off-specular reflectivity of polarized neutrons was used to study magnetization reversal in an array of micron-sized ferromagnetic islands.[19] Here, we calculate how the impurity-spin magnetization is affected by the shape-dependent surface-induced anisotropy and analyze the possibility to detect this magnetization in the polarized-neutron reflectivity of thin polycrystalline films of homogeneous dilute magnetic alloys.

II. FORMALISM

In a grain subjected to a magnetic field **B**, the thermodynamic average for the impurity-spin component along **B** can be written as[6,11,12]

$$\langle S_B\rangle = -\frac{1}{2\mu_B\mathcal{Z}}\sum_{k=1}^{2S+1}\exp\left(-\frac{E_k}{k_BT}\right)\frac{dE_k}{dB}, \tag{1}$$

where S is the impurity spin and μ_B is the Bohr magneton. The Landé factor of the electron is assumed to be 2 and the partition function $\mathcal{Z}$ is defined as $\mathcal{Z}=\Sigma_{k=1}^{2S+1}\exp(-E_k/k_BT)$. The index $k=1,\ldots,2S+1$ labels the roots E_k of the secular equation

$$\left|H_{S_B'S_B}-E\,\delta_{S_B'S_B}\right|=0 \quad (S_B,S_B'=-S,\ldots,S), \tag{2}$$

with the Hamiltonian

$$H=-2\mu_B\mathbf{S}\cdot\mathbf{B}+H_{an}, \tag{3}$$

where **S** is the impurity-spin operator. The Hamiltonian H_{an} describes the surface-induced magnetic anisotropy for an im-

purity spin. This anisotropy is caused by the interaction of the magnetic impurity with conduction electrons, which undergo spin-orbit scattering by nonmagnetic host atoms. In Refs. 7 and 8, an explicit expression for the Hamiltonian $H_{\rm an}$ was obtained for the case of magnetic impurities in a semi-infinite nonmagnetic host. The method, suggested in Refs. 10–12 and briefly described below, allows one to derive $H_{\rm an}$ for samples with more complicated shapes.

To the lowest order in the electron-impurity and spin-orbit interaction, the anisotropic contribution to the self-energy of the impurity spin arises from the fundamental process[7,8] involving the spin-orbit scattering of an electron by two host atoms. Denoting this contribution as $\Phi(\mathbf{R},\mathbf{R}')$, where $\mathbf{R}$ and $\mathbf{R}'$ are radius vectors of the two host atoms in a coordinate frame with the origin at the magnetic impurity, the Hamiltonian $H_{\rm an}$ is expressed as

$$H_{\rm an} = \frac{1}{a^6} \int\limits_{\rm grain} {\rm d}^3R \int\limits_{\rm grain} {\rm d}^3R' \Phi(\mathbf{R},\mathbf{R}'), \tag{4}$$

where a^3 is the volume per host atom and the integrations are performed over all possible positions of host atoms within the grain. It is convenient to rewrite Eq. (4) in the form

$$H_{\rm an} = \frac{1}{a^6} \Bigg[\int\limits_{\substack{\rm whole \\ \rm space}} {\rm d}^3R \int\limits_{\substack{\rm whole \\ \rm space}} {\rm d}^3R' \Phi(\mathbf{R},\mathbf{R}') + \int\limits_{\substack{\rm outer \\ \rm domain}} {\rm d}^3R \int\limits_{\substack{\rm outer \\ \rm domain}} {\rm d}^3R' \Phi(\mathbf{R},\mathbf{R}') - 2 \int\limits_{\substack{\rm outer \\ \rm domain}} {\rm d}^3R \int\limits_{\substack{\rm whole \\ \rm space}} {\rm d}^3R' \Phi(\mathbf{R},\mathbf{R}') \Bigg], \tag{5}$$

where the first term on the right-hand side is obviously isotropic and can be omitted. For $Rk_{\rm F} > 1$ ($R'k_{\rm F} > 1$), where $k_{\rm F}$ is the Fermi wave number of conduction electrons, the function $\Phi(\mathbf{R},\mathbf{R}')$ rapidly decreases with increasing R (R') because of a decrease of the overlap integral between spherical waves centered at R (R') and at the magnetic impurity.[8] Therefore, assuming that the distance d between the magnetic impurity and the nearest element of the grain surface significantly exceeds[13] $k_{\rm F}^{-1}$, the second term on the right-hand side of Eq. (5) can be neglected when compared to the third one. In the latter term, we choose for the "primed" host atoms a coordinate frame with the z-axis parallel to $\mathbf{R}$, obtaining

$$H_{\rm an} = -2 \int_0^{2\pi} {\rm d}\varphi \int_0^{\pi} {\rm d}\vartheta \, \sin\vartheta (\mathbf{e}(\vartheta,\varphi)\cdot\mathbf{S})^2 I(\vartheta,\varphi), \tag{6}$$

$$I(\vartheta,\varphi) = \int_{R_f(\vartheta,\varphi)}^{\infty} {\rm d}R R^2 \int_0^{\pi} {\rm d}\vartheta' \, \sin\vartheta' \times \int_0^{\infty} {\rm d}R' R'^2 \phi(R,0,R',\vartheta'), \tag{7}$$

where $\mathbf{e}(\vartheta,\varphi)$ is the unit vector in the $\mathbf{R}$-direction, $R = R_f(\vartheta,\varphi)$ describes the grain surface, and the function $\phi(R,\vartheta,R',\vartheta')$ is given by expression (27) of Ref. 8. To leading order in the (small) parameter $1/(dk_{\rm F})$, one finds

$$I(\vartheta,\varphi) = -\frac{2A}{\pi k_{\rm F} R_f(\vartheta,\varphi)}, \tag{8}$$

where A is the material-dependent anisotropy-strength constant.[8,10] Using the relation ${\rm d}\varphi{\rm d}\vartheta \sin\vartheta = {\rm d}\mathbf{f}\cdot\mathbf{e}(\vartheta,\varphi)/R_f^2(\vartheta,\varphi)$, where ${\rm d}\mathbf{f}$ is the grain-surface element with coordinates $(R_f(\vartheta,\varphi),\vartheta,\varphi)$, we finally obtain[12]

$$H_{\rm an} = \frac{4A}{\pi k_{\rm F}} \int_{\rm surface} {\rm d}\mathbf{f}\cdot\mathbf{R}_f \frac{(\mathbf{R}_f\cdot\mathbf{S})^2}{R_f^6}. \tag{9}$$

The integration is performed over the surface of the grain, and $\mathbf{R}_f$ is the radius vector drawn from the impurity site to the surface element ${\rm d}\mathbf{f}$.

Next, we analyze the specular reflection of neutrons by films of dilute magnetic alloys for the case when the applied magnetic field $\mathbf{B}$ is parallel to the surface of the film, using the transfer matrix formalism.[14,20] Equations (1)–(3) and (9) allow us to find the position-dependent impurity-spin component $\langle S_B\rangle$ in a grain of arbitrary shape and then to calculate the magnetization profiles across a film that can be probed by the neutron reflectivity measurements. In a single-crystal film, where the surface-induced anisotropy forms for impurity spins an easy plane parallel to the film surface, the thermodynamic average of the impurity-spin magnetic moment, $2\mu_{\rm B}\langle\mathbf{S}\rangle$, is always aligned with the applied magnetic field. Because of the competing influence of film surfaces and differently oriented interfaces between grains on the impurity-spin magnetic anisotropy, the condition $\langle\mathbf{S}\rangle\|\mathbf{B}$ may be violated for an impurity in a polycrystalline film when the distance between this impurity and an interface between grains is comparable with or smaller than the film thickness t. Hence, in grains with lateral sizes as small as a few nanometers, i.e., for the granular films under consideration (in Sec. III calculations are performed for granular films with $t = 30$ nm), a certain fraction of impurities may have magnetic moments that are not parallel to the magnetic field $\mathbf{B}$. However, when averaging the impurity-spin magnetic moments over the surface area that is coherently probed by neutron-reflectivity measurements (typically of the order of tens of micrometers)[21,22] the averaged magnetization is parallel to $\mathbf{B}$ in a film with randomly oriented grains, due to symmetry reasons. The same also holds for films with an ordered orientation of grains, which provides an in-plane symmetry axis, when the applied magnetic field is parallel to that axis. Below, we assume that one of the above two cases occurs.

For simplicity, we neglect surface roughness as well as the neutron-beam angular divergence. More detailed calculations reveal that for realistic values of the surface roughness and beam divergence, the conclusions presented below remain unaffected. The vacuum-film-substrate structure is modeled as an N-layer system, the first (semi-infinite) layer being the vacuum and the Nth (semi-infinite) layer being the nonmagnetic substrate. The film is subdivided into $N-2$ thin layers labeled by the index j ($j = 2,\ldots,N-1$). Within each of these layers, the impurity-spin magnetization $\langle S_B\rangle_j$ is ap-

proximated by the value $[\langle S_B\rangle]_{cs}$ obtained by averaging the local magnetization $\langle S_B\rangle$ over the middle cross section of the layer.

Since the magnetization is aligned with the applied magnetic field, the reflected intensity of the neutron beam can be written as[14,20]

$$R^{\pm} = \left| \frac{M_{21}^{\pm}}{M_{11}^{\pm}} \right|^2, \tag{10}$$

where the superscripts "+" (spin up) and "−" (spin down) stand for neutrons with spins parallel and antiparallel to the magnetic field, respectively. The transfer matrix $\hat{M}^{\pm}$ is given by

$$\hat{M}^{\pm} = \hat{D}^{-1}(q_1^{\pm}) \left\{ \prod_{j=2}^{N-1} [\hat{D}(q_j^{\pm}) \hat{P}(q_j^{\pm}, d_j) \hat{D}^{-1}(q_j^{\pm})] \right\} \hat{D}(q_N^{\pm}) \tag{11}$$

with transmission matrices

$$\hat{D}(q) = \begin{pmatrix} 1 & 1 \\ q & -q \end{pmatrix} \tag{12}$$

and propagation matrices

$$\hat{P}(q,d) = \begin{pmatrix} e^{-iqd} & 0 \\ 0 & e^{iqd} \end{pmatrix}. \tag{13}$$

In Eq. (11), d_j is the thickness of the jth layer, while $q_j^{\pm}$ is the transverse component of the neutron wave vector

$$q_j^{\pm} = \left\{ \left(\frac{2\pi}{\lambda} \right)^2 - 4\pi\rho_j b_j \pm \frac{2mg_n\mu_n}{\hbar^2} B_j - \left[\left(\frac{2\pi}{\lambda} \right)^2 \pm \frac{2mg_n\mu_n}{\hbar^2} B \right] \cos^2\theta \right\}^{1/2}, \tag{14}$$

where λ is the neutron wavelength, θ is the angle between the incident neutron beam and the surface of the film, ρ_j and b_j are the atomic density and the coherent neutron-scattering length of the jth layer, respectively, m is the neutron mass, $g_n = -1.9132$ is the Landé factor of the neutron, and μ_n is the nuclear magneton. The effective in-plane magnetic field in the jth layer B_j coincides with B for $j=1$ and $j=N$, while for $j=2,\ldots,N-1$, it is given by

$$B_j = B + 2\mu_0\mu_B\rho_j^{\text{imp}}\langle S_B\rangle_j, \tag{15}$$

where μ_0 is the permeability of the vacuum and ρ_j^{imp} is the atomic density of magnetic impurities in the jth layer of the film. Assuming that the magnetic alloy is sufficiently dilute, we use for ρ_j^{imp} the expression $\rho_j^{\text{imp}} = c_j^{\text{imp}}\rho^{\text{host}}$, with c_j^{imp} the atomic concentration of magnetic impurities and ρ^{host} the atomic density of the undoped host medium. Taking into account Eq. (15), we can rewrite Eq. (14) in the form

$$q_j^{\pm} = \left[\frac{Q^2}{4} - 4\pi\rho_j b_j \pm \frac{4mg_n\mu_n\mu_0\mu_B\rho_j^{\text{imp}}}{\hbar^2}\langle S_B\rangle_j \right]^{1/2}, \tag{16}$$

where $Q = 4\pi\lambda^{-1}\sin\theta$ is the momentum transfer for reflected neutrons.

Once the values $\langle S_B\rangle_j$ of the impurity-spin magnetization have been calculated, Eqs. (10)–(13) together with Eq. (16) completely determine the neutron-reflectivity coefficients R^+ and R^- for the structure under consideration. Below, we will analyze the spin asymmetry s, which is defined as

$$s = \frac{R^+ - R^-}{R^+ + R^-} \tag{17}$$

and reflects the difference in reflectivity for spin-up and spin-down neutrons. As can be seen from Eqs. (10), (11), and (16), this normalized difference is sensitive to the magnetization profile across the film.

III. RESULTS AND DISCUSSION

Let us now consider the impurity-spin magnetization and the neutron reflectivity for thin Fe-doped Au films that consist of parallelepiped-shaped grains and are deposited on a semi-infinite nonmagnetic substrate. In order to reduce the number of input parameters, we assume that all grains within a film are equal and, moreover, have an identical orientation. The grain edges are taken parallel to the axes of a Cartesian coordinate frame. The z-axis is assumed to be perpendicular to the film. Consequently, the height of the grains a_z coincides with the film thickness, which is chosen to be 30 nm in the calculations below. The lateral grain sizes are a_x and a_y.

For an arbitrary position (x,y,z) of a magnetic impurity in a parallelepiped-shaped grain, the integration over the grain surface in Eq. (9) can be performed analytically, leading for the Hamiltonian H_{an} to an expression of the form

$$\begin{aligned} H_{\text{an}} = A[&S_x^2 b(x,y,z) + S_y^2 b(y,x,z) + S_z^2 b(z,x,y) \\ &+ (S_x S_y + S_y S_x) c(x,y,z) + (S_x S_z + S_z S_x) c(x,z,y) \\ &+ (S_y S_z + S_z S_y) c(y,z,x)] \end{aligned} \tag{18}$$

with the functions $b(\xi,\eta,\zeta)$ and $c(\xi,\eta,\zeta)$ $(\xi,\eta,\zeta = x,y,z)$ explicitly given in Refs. 11 and 12. For the anisotropy-strength constant in dilute AuFe alloys, a value $A = 0.12$ eV was inferred[6] from a comparison between theoretical and experimental data for the anomalous Hall effect in thin AuFe films. We use the aforementioned results[6,11,12] to calculate the position-dependent magnetization $\langle S_B\rangle$ of an Fe spin ($S=2$) in AuFe grains. Next, the impurity-spin magnetization $\langle S_B\rangle$ is averaged over all positions of impurities within a cross section parallel to the film surface. This average, $[\langle S_B\rangle]_{cs}$, as a function of the distance between the cross section and the film surface, represents the magnetization profile across the film.

In Fig. 1 we show the calculated magnetization $[\langle S_B\rangle]_{cs}$ as a function of the distance between the cross section and the film surface for grains with different lateral size (grains with a square base, $a_x = a_y$, are considered). The calculations are performed for a temperature $T = 1$ K and a magnetic field $B = 1$ T, which is taken parallel to the x-axis. Due to the surface-induced magnetic anisotropy, the magnetization of impurity spins rapidly decreases when the cross section under consideration approaches the surface of the film. Even in the middle of the film, the magnetization remains signifi-

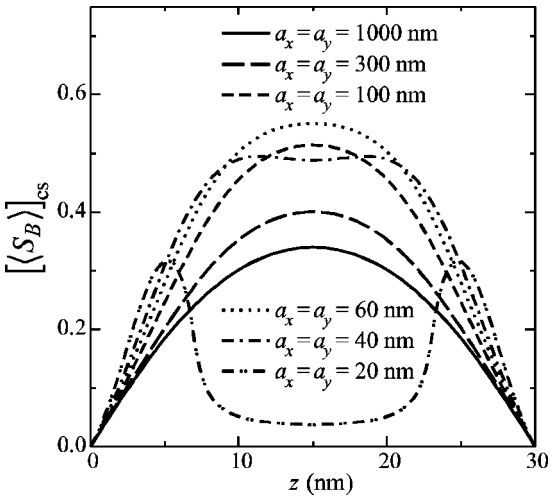

FIG. 1. Cross-section average for the magnetization of impurities in parallelepiped-shaped AuFe grains, $[\langle S_B \rangle]_{cs}$, as a function of the distance between the cross section and the film surface, which is taken to lie in the *xy* plane. Different curves are for different lateral size of grains with square base ($a_x = a_y$). The height of the grains, $a_z = 30$ nm, coincides with the film thickness. The magnetic field, $B = 1$ T, is parallel to the *x*-axis. Calculations are performed for a temperature $T = 1$ K and an anisotropy-strength constant $A = 0.12$ eV.

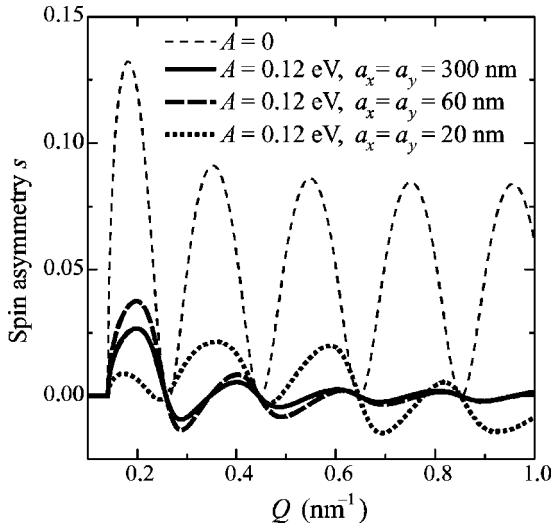

FIG. 2. Spin asymmetry, calculated for polycrystalline AuFe films with an Fe concentration of 2 at. % on a semi-infinite SiO_2 substrate, as a function of the neutron momentum transfer Q. Results are shown for the case of vanishing surface-induced anisotropy ($A = 0$, thin dashed curve) and for the case $A = 0.12$ eV with different lateral grain size (thick curves). The height of the grains, $a_z = 30$ nm, coincides with the film thickness. The magnetic field, $B = 1$ T, is parallel to the *x*-axis. Calculations are performed for $T = 1$ K.

cantly smaller than its bulk value, which is 1.653 at the considered values of T, B, and S. A less trivial result is the substantial difference, revealed by our calculations, between the magnetization profile in flat grains (with a_x and a_y significantly larger than a_z) on one hand, and that in pillarlike (with $a_x, a_y < a_z$) and nearly cubic grains on the other hand. In the latter case, the maximum magnetization is clearly shifted from the middle cross section toward the surface. Based on the results shown in Fig. 1, we also conclude that the magnetization averaged over the whole grain is a nonmonotonous function of the lateral size of the grain. When modifying the grain shape from pillarlike to flat, this average magnetization first increases, next reaches a maximum at $a_x, a_y \approx 40$ to 60 nm, and finally decreases, approaching a nonzero limiting value at $a_x, a_y \to \infty$ (the limit of a single-crystal film).

In Fig. 2 the spin asymmetry *s*, calculated for AuFe films on a semi-infinite nonmagnetic substrate, is plotted as a function of the neutron momentum transfer Q for films with different lateral grain sizes. For the SiO_2 substrate the following parameters[14] are used: $\rho_N = \rho^{SiO_2} = 25.1$ nm^{-3}, $b_N = b^{SiO_2} = 15.8 \times 10^{-6}$ nm. The atomic concentration of Fe in the AuFe films is assumed to be homogeneous: $c_j^{Fe} = 2$ at. % for $j = 2, \ldots, N-1$. For the atomic density of these layers, the density of pure Au is used[14] : $\rho_j = \rho^{Au} = 59$ nm^{-3}. The scattering length is assumed to be $b_j = c_j^{Fe} b^{Fe} + (1 - c_j^{Fe}) b^{Au}$, where[14] $b^{Fe} = 9.45 \times 10^{-6}$ nm and $b^{Au} = 7.63 \times 10^{-6}$ nm. The spin asymmetry in the absence of the surface-induced anisotropy ($A = 0$) is also shown. At any lateral size of grains under consideration, the surface-induced anisotropy is seen to substantially reduce the amplitude of the oscillations of *s* versus Q when compared to the case of $A = 0$. At the same time, the detailed shape of these oscillations is appreciably different for different values of a_x and a_y, reflecting the corresponding differences between the magnetization profiles in grains with various lateral sizes (see Fig. 1).

Figure 3 displays the spin asymmetry calculated for one

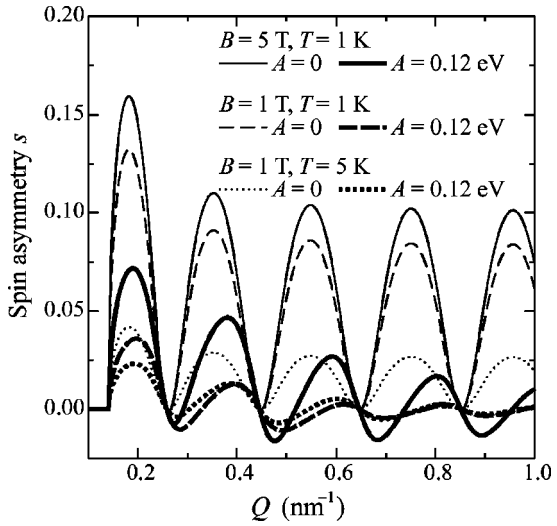

FIG. 3. Spin asymmetry, calculated for a polycrystalline AuFe film with an Fe concentration of 2 at. % on a semi-infinite SiO_2 substrate, as a function of the neutron momentum transfer Q at different magnetic fields B and temperatures T. Results are shown for the case of vanishing surface-induced anisotropy ($A = 0$, thin curves) and for the case of $A = 0.12$ eV (thick curves). The lateral size of the grains is $a_x = a_y = 40$ nm, while their height, $a_z = 30$ nm, coincides with the film thickness. The magnetic field is parallel to the *x*-axis.

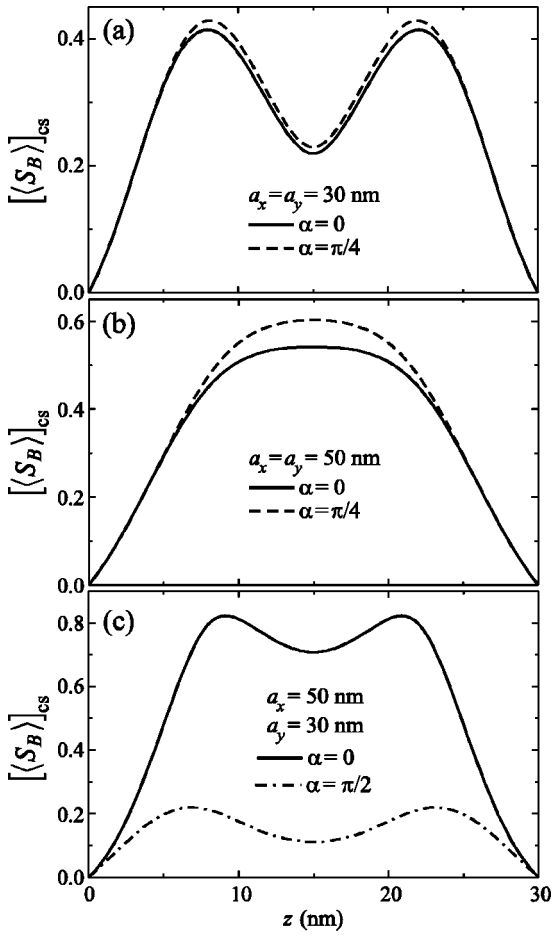

FIG. 4. Cross-section average for the magnetization of impurities in parallelepiped-shaped AuFe grains, $[\langle S_B \rangle]_{cs}$, as a function of the distance between the cross section and the surface of the film, which is taken to lie in the *xy* plane. Different curves are for different angles α between the direction of the applied magnetic field, which lies in the plane of the film, and the *x*-axis. Calculations are performed for a temperature $T=1$ K, a magnetic field $B=1$ T, an anisotropy-strength constant $A=0.12$ eV, and different lateral sizes of the grains. The height of the grains, $a_z=30$ nm, coincides with the film thickness.

particular AuFe film at different values of *T* and *B*. From Fig. 3 we conclude that the suppression by the surface-induced anisotropy of the spin asymmetry remains quite strong in a rather wide range of temperatures and magnetic fields, although it becomes relatively less pronounced with increasing *T* or *B*.

We now address the question how the magnetization profiles and the spin asymmetry depend on the orientation of the in-plane magnetic field with respect to the grain edges. We assume that the magnetic field is directed along one of the symmetry axes of the grain and forms an angle α with the *x*-axis. In Figs. 4(a) and 4(b) the magnetization profiles are shown at $\alpha=0$ and $\alpha=\pi/4$ for a cubic grain and for a flat grain with a square base ($a_x=a_y=50$ nm), respectively. Figures 4(a) and 4(b) imply that for both types of grains the dependence of the magnetization on α is weak. However, the situation dramatically changes when the shape of the grain base in the *xy* plane substantially deviates from a square. In

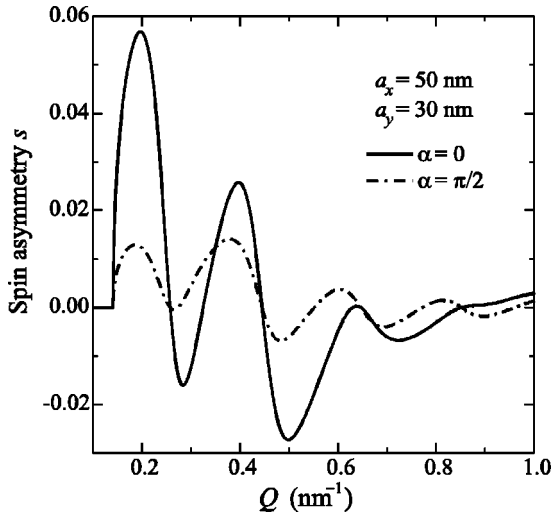

FIG. 5. Spin asymmetry, calculated for a polycrystalline AuFe film with an Fe concentration of 2 at.% on a semi-infinite SiO_2 substrate, as a function of the neutron momentum transfer *Q* for an in-plane applied magnetic field parallel ($\alpha=0$) and perpendicular ($\alpha=\pi/2$) to the *x*-axis. The film is considered to consist of parallelepiped-shaped AuFe grains with lateral sizes $a_x=50$ nm and $a_y=30$ nm. The height of grains, $a_z=30$ nm, coincides with the film thickness. Calculations are performed for a temperature $T=1$ K, a magnetic field $B=1$ T and an anisotropy-strength constant $A=0.12$ eV.

Fig. 4(c), the magnetization profiles are plotted for a grain with $a_x=50$ nm and $a_y=30$ nm. For most of the impurities in this grain, the magnetic anisotropy is dominated by the effect of grain surfaces parallel to the *x*-axis (total area of these surfaces is substantially larger than that of surfaces perpendicular to the *x*-axis). Due to a combined effect of the four "large" surfaces, impurity spins tend to be aligned parallel to the *x*-axis. As a result, the impurity-spin magnetization $[\langle S_B \rangle]_{cs}$ reaches its maximum value for a magnetic field **B** parallel to the *x*-axis and significantly decreases when rotating **B** toward the *y*-axis.

In Fig. 5 we show the spin asymmetry *s* versus the momentum transfer *Q* for neutron reflection by a film that consists of laterally anisotropic grains with $a_x=50$ nm and $a_y=30$ nm. As before, the neutron spins are assumed to be either parallel or antiparallel to the applied magnetic field. As expected from the above results for the magnetization profiles, the oscillation amplitudes of *s* versus *Q* strongly decrease when changing α from 0 (magnetic field parallel to the long axis of the grains) to $\pi/2$ (magnetic field parallel to the short axis of the grains). It is worth noting that this effect becomes more pronounced for small *Q* (i.e., at small angles between the incident neutron beam and the surface of the film), where the reflected intensity of the neutron beam is sufficiently high. Obviously, the described effect cannot be observed in films with a completely random orientation of grains. However, our calculations imply that a strong dependence of the neutron-spin asymmetry on the orientation of an in-plane magnetic field can be observed when, in addition to an anisotropy of the lateral shape of grains, there also exists a preferred orientation for the long axis of the grains in the

film plane. Experimentally, it might be possible to grow films with such an anisotropic microstructure using an appropriate substrate and appropriate deposition conditions,[23,24] or by using lithographic methods.

IV. CONCLUSIONS

We have shown that the surface-induced anisotropy reduces the magnetization of impurity spins. We find that the reduced magnetization results in a weaker spin asymmetry in the polarized-neutron reflectivity of thin polycrystalline AuFe films. This effect remains pronounced for a wide range of temperatures and magnetic fields.

Our calculations reveal a qualitative difference between the magnetization profiles in films with flat grains and the profiles in films consisting of pillarlike or nearly cubic grains. Consequently, the spin asymmetry as a function of the momentum transfer becomes sensitive to the shape of the grains forming the film.

For films with a laterally anisotropic microstructure, the spin asymmetry is shown to strongly depend on the orientation of an in-plane magnetic field. Polarized-neutron reflectivity measurements on such films will provide a direct probe of the surface-induced magnetic anisotropy of impurity spins in dilute magnetic alloys.

ACKNOWLEDGMENTS

We would like to thank H. Fritzsche for enlightening discussions. This work has been supported by the Concerted Action (Geconcerteerde Onderzoeksactie) and the Interuniversity Attraction Poles (Interuniversitaire Attractiepolen) research programs. Support has also been provided by the Fund for Scientific Research–Flanders (Fonds voor Wetenschappelijk Onderzoek–Vlaanderen): projects G.0435.03 and G.0449.04, Scientific Research Community (Wetenschappelijke Onderzoeksgemeenschap, WOG) WO.025.99 (Belgium).

*Permanent address: Department of Theoretical Physics, State University of Moldova, Str. A. Mateevici 60, MD-2009 Kishinev, Republic of Moldova.

†Also at: COBRA, Technische Universiteit Eindhoven, P. O. Box 513, 5600 MB Eindhoven, The Netherlands.

[1] G. Chen and N. Giordano, Phys. Rev. Lett. **66**, 209 (1991).

[2] J. F. DiTusa, K. Lin, M. Park, M. S. Isaacson, and M. Parpia, Phys. Rev. Lett. **68**, 1156 (1992).

[3] V. Chandrasekhar, P. Santhanam, N. E. Penebre, R. A. Webb, H. Vloeberghs, C. Van Haesendonck, and Y. Bruynseraede, Phys. Rev. Lett. **72**, 2053 (1994).

[4] M. A. Blachly and N. Giordano, Phys. Rev. B **51**, 12 537 (1995).

[5] C. Strunk, M. Henny, C. Schönenberger, G. Neuttiens, and C. Van Haesendonck, Phys. Rev. Lett. **81**, 2982 (1998).

[6] E. Seynaeve, K. Temst, F. G. Aliev, C. Van Haesendonck, V. N. Gladilin, V. M. Fomin, and J. T. Devreese, Phys. Rev. Lett. **85**, 2593 (2000).

[7] O. Újsághy, A. Zawadowski, and B. L. Gyorffy, Phys. Rev. Lett. **76**, 2378 (1996).

[8] O. Újsághy and A. Zawadowski, Phys. Rev. B **57**, 11 598 (1998).

[9] O. Újsághy and A. Zawadowski, Phys. Rev. B **57**, 11 609 (1998).

[10] V. M. Fomin, V. N. Gladilin, J. T. Devreese, C. Van Haesendonck, and G. Neuttiens, Solid State Commun. **106**, 293 (1998).

[11] V. N. Gladilin, V. M. Fomin, and J. T. Devreese, Physica B **294–295**, 302 (2001).

[12] V. N. Gladilin, V. M. Fomin, and J. T. Devreese, in *Kondo Effect and Dephasing in Low-Dimensional Metallic Systems*, edited by V. Chandrasekhar, C. Van Haesendonck, and A. Zawadowski (Kluwer, Dordrecht, 2001), pp. 43–52.

[13] There are two reasons for not taking into account the magnetic impurities with $d \lesssim k_F^{-1}$. (i) Even in small grains with sizes $\sim$10 nm, only a small fraction of impurities are within a layer of width $\sim k_F^{-1}$ near the surface. (ii) Due to a strong surface-induced anisotropy, the magnetization $\langle S_B \rangle$ of those impurities is negligibly small when compared to the average magnetization of impurities within the grain.

[14] C. Fermon, F. Ott, and A. Menelle, in *X-Ray and Neutron Reflectivity: Principles and Applications*, edited by J. Daillant and A. Gibaud (Springer, Berlin, 1999), pp. 163–195.

[15] G. P. Felcher, J. Appl. Phys. **87**, 5431 (2000).

[16] S. M. Yusuf, R. M. Osgood, J. S. Jiang, C. H. Sowers, S. D. Bader, E. E. Fullerton, and G. P. Felcher, J. Magn. Magn. Mater. **199**, 564 (1999).

[17] M. P. Nutley, A. T. Boothroyd, C. R. Staddon, D. McK. Paul, and J. Penfold, Phys. Rev. B **49**, 15 789 (1994).

[18] H. Zabel and K. Theis-Bröhl, J. Phys.: Condens. Matter **15**, S505 (2003).

[19] K. Temst, M. J. Van Bael, and H. Fritzsche, Appl. Phys. Lett. **79**, 991 (2001).

[20] S. J. Blundell and J. A. C. Bland, Phys. Rev. B **46**, 3391 (1992).

[21] B. P. Toperverg, Physica B **297**, 160 (2001).

[22] C. H. Marrows, S. Langridge, M. Ali, A. T. Hindmarch, D. T. Dekadjevi, S. Foster, and B. J. Hickey, Phys. Rev. B **66**, 024437 (2002).

[23] S. van Dijken, L. C. Jorritsma, and B. Poelsema, Phys. Rev. B **61**, 14 047 (2000).

[24] S. van Dijken, G. Di Santo, and B. Poelsema, Phys. Rev. B **63**, 104431 (2001).